



**HAL**  
open science

## **Clay mineral distributions in and around the Mississippi River watershed and Northern Gulf of Mexico: sources and transport patterns**

T Sionneau, Viviane Bout-roumazeilles, P E Biscaye, B van Vliet-Lanoe, A Bory

### **► To cite this version:**

T Sionneau, Viviane Bout-roumazeilles, P E Biscaye, B van Vliet-Lanoe, A Bory. Clay mineral distributions in and around the Mississippi River watershed and Northern Gulf of Mexico: sources and transport patterns. *Quaternary Science Reviews*, 2008, 27 (17-18), pp.1740-1751. <hal-03290439>

**HAL Id: hal-03290439**

**<https://hal.science/hal-03290439v1>**

Submitted on 19 Jul 2021

**HAL** is a multi-disciplinary open access archive for the deposit and dissemination of scientific research documents, whether they are published or not. The documents may come from teaching and research institutions in France or abroad, or from public or private research centers.

L'archive ouverte pluridisciplinaire **HAL**, est destinée au dépôt et à la diffusion de documents scientifiques de niveau recherche, publiés ou non, émanant des établissements d'enseignement et de recherche français ou étrangers, des laboratoires publics ou privés.



HAL Authorization

# 1 Clay mineral distributions in and around the Mississippi River watershed 2 and Northern Gulf of Mexico: sources and transport patterns

3  
4 T. Sionneau <sup>a,\*</sup>, V. Bout-Roumazeilles <sup>a</sup>, P.E. Biscaye <sup>b</sup>, B. Van Vliet-Lanoe <sup>c</sup>, A. Bory <sup>a,b</sup>

5  
6 <sup>a</sup> UMR CNRS 8157 “Géosystèmes”, Université de Lille 1, Bât. SN5, Cité Scientifique,  
7 59655 Villeneuve d’Ascq Cedex, France

8 <sup>b</sup> Lamont–Doherty Earth Observatory of Columbia University, Palisades, NY 10964, USA

9 <sup>c</sup> UMR 6538 CNRS, Domaines Océaniques, IUEM, 29280 Plouzané, France

10 \*Corresponding author. Tel.: +33 3 20 43 70 38; fax: +33 3 20 43 49 10. E-mail address:

11 [thomas.sionneau@ed.univ-lille1.fr](mailto:thomas.sionneau@ed.univ-lille1.fr) (T. Sionneau).

## 12 13 **Abstract**

14 Maps of the distributions of the four major clay minerals (smectite, illite, kaolinite and  
15 chlorite) in and around the Mississippi River drainage basin and in the Northern Gulf of  
16 Mexico have been produced using newly acquired data from erodible/alluvial terrestrial  
17 sediments and marine surface sediments, as well as from previously published data. East of  
18 the Rockies, North America can be divided into four, large, clay-mineral provinces: (1) the  
19 north-western Mississippi River watershed (smectite rich), (2) the Great Lakes area and  
20 eastern Mississippi River watershed (illite and chlorite rich), (3) the south-eastern United  
21 States (kaolinite rich) and (4) the Brazos River and south-western Mississippi River  
22 watersheds (illite and kaolinite rich). The clay mineral distributions in surface sediments of  
23 the present-day Gulf of Mexico are strongly influenced by three main factors: (1) by relative  
24 fluvial contributions: the Mississippi River delivers the bulk of the clay input to the Northern  
25 Gulf of Mexico whereas the Apalachicola, Mobile, Brazos and Rio Grande rivers inputs have  
26 more local influences; (2) by differential settling of various clay mineral species, which is  
27 identified for the first time in Northern Gulf of Mexico sediments; and (3) by oceanic current  
28 transport: the Gulf of Mexico surface and subsurface circulation distributes the clay-rich  
29 sediments from river mouth sources throughout the Northern Gulf of Mexico.

## 30 31 **1. Introduction**

32 Clay minerals are a dominant component of most marine sediments, and are mainly  
33 land-derived (Biscaye, 1965; Griffin et al., 1968). Their geographic distributions and sources

34 have been extensively investigated since the 1960s (Biscaye, 1965; Griffin and  
35 Goldberg, 1969; Rateev et al., 1969; Gradusov, 1974; Windom, 1976). Studies of clay mineral  
36 assemblages provide information on climatic conditions, such as precipitation and runoff  
37 patterns over the adjacent continents (Chamley, 1989), as well as on the dynamics of river  
38 inputs (Pinsak and Murray, 1960; Scafe and Kunze, 1971; Doyle and Sparks, 1980). Clay  
39 minerals can be advected over long distances and then settle far away from their source area,  
40 especially if being re-transported in the nepheloid layer (Biscaye and Eittrheim, 1977; Jones,  
41 1984). Thus, clay mineral assemblages have also been successfully used to trace oceanic  
42 current patterns (Petschick et al., 1996; Fagel et al., 1997; Gingele et al., 2001; Boulay et al.,  
43 2005).

44         The Gulf of Mexico has been an important area for global thermohaline circulation  
45 and for the global climatic system (Broecker, 1991) especially since the closure of the  
46 Isthmus of Panama 4.6 million years ago (Haug and Tiedemann, 1998). Gulf of Mexico  
47 surface waters are characterized by high temperature and high salinity that further influence  
48 the Gulf Streamwater properties. The hydrological features of the Gulf of Mexico were  
49 strongly modified by the inputs of freshwater resulting from melting pulses of the Laurentide  
50 Ice Sheet (LIS) during the last glacial cycle and the last deglaciation (Kennett and Shackleton,  
51 1975; Leventer et al., 1982; Joyce et al., 1993; Aharon, 2003; Flower et al., 2004). Changes of  
52 salinity resulting from these melting pulses are thought to have altered the thermohaline  
53 circulation, the global heat exchange and worldwide climatic conditions (Broecker et al.,  
54 1990; Bond, 1995; Rahmstorf, 1995; Manabe and Stouffer, 1997). Although the direct  
55 palaeoceanographic effects of these freshwater supplies on the Gulf of Mexico have been  
56 studied largely using  $\delta^{18}\text{O}$  variations, the associated terrigenous inputs (mostly clay minerals;  
57 Brown and Kennett, 1998) have been poorly investigated. They may, however, provide  
58 information on the varying continental provenance of these freshwater pulses and therefore  
59 help close the gap between climate variations over the continent (e.g. the dynamics of the  
60 LIS/ proglacial lake overflows and/or increase in precipitation; Broecker et al., 1989; Teller,  
61 1995; Clark et al., 2001; Clarke et al., 2003) and the hydrological changes in the Gulf of  
62 Mexico. In order to use clay mineral records from the Gulf of Mexico for palaeoclimate  
63 reconstructions (Sionneau et al., in preparation), one must have a good knowledge of clay  
64 mineral continental sources and of the factors influencing their distribution in the Gulf of  
65 Mexico. It seems reasonable to assume that the nature of the main clay mineral provinces in  
66 North America has remained unchanged during the late Quaternary. Variations in clay  
67 mineral assemblages in the Gulf of Mexico surface sediments are then mainly controlled by

68 changes in erosion and transport pattern, even if their intrinsic nature derived from weathering  
69 processes developed over longer timescale (Thiry et al., 1999; Thiry, 2000).

70 The present Gulf of Mexico circulation pattern is relatively well known (Fig. 1). Its  
71 sedimentology has been extensively studied (Griffin, 1962; Doyle and Sparks, 1980; Balsam  
72 and Beeson, 2003; Ellwood et al., 2006). None of these studies, however, combined data from  
73 both continental and marine environments, and no overall clay mineral distributions over  
74 North America and the Northern Gulf of Mexico are available today.

75 In this paper, we present the clay mineral assemblage of 28 continental sites  
76 [consisting of 85 new samples and data from Griffin (1962) and Potter et al. (1975)] over  
77 North America and of 67 core-top samples collected over the Northern Gulf of Mexico. The  
78 main objectives of this study are: (1) to map clay mineral distributions over both the North  
79 American continent east of the Rockies and the Northern Gulf of Mexico; (2) to discern and  
80 distinguish the continental sources of the principal marine clay minerals; and (3) to identify  
81 the main parameters (fluvial contributions, differential settling, oceanic currents) controlling  
82 the present-day marine distribution of these clay minerals in the Northern Gulf of Mexico.

83

## 84 **2. Samples**

85 Marine core-top samples were recovered during the RVs Robert Conrad (RC), Vema  
86 (VM) and Atlantis (AT) cruises (Lamont core collection; Table 1; samples 13–67) as well as  
87 during the RV Marion Dufresne IMAGES cruise PAGE in 2002 (Bout-Roumazelles and  
88 Trentesaux, 2006; samples 3–12) and PICASSO in 2003 (Laj et al., 2004; samples 1 and 2).  
89 They are broadly distributed over the northern Gulf of Mexico (Fig. 2) and are located within  
90 the different geomorphologic provinces that characterize this area (Fig. 3).

91 Over the North American continent, 85 samples were collected from different types of  
92 sediment (loess, recent mineral dust deposits, tills, lake and river) at 14 sites (Fig. 4, Table 2).  
93 Sediment samples of fluvial origin were taken from the C horizon of alluvial plain soils  
94 (about 1.5–2 m depth) from which, except for the carbonate content, the mineralogical  
95 composition is not likely to have been disturbed by anthropogenic activity and should reflect  
96 the bulk composition of superficial deposits such as loess, alluvium or tills (Gallet et al.,  
97 1998). All these continental samples are commonly representative of the regional and/or  
98 upstream watershed average mineralogical composition. In addition we have included  
99 published clay mineral data from 11 sites on the Mississippi river system (Potter et al., 1975)  
100 and from the Mobile Embayment, the Mississippi and the Apalachicola River mouths (Fig. 5,  
101 Table 2; Griffin, 1962). The majority of the continental sites (20 of 28) are located in the

102 present-day Mississippi River watershed (Fig. 4).

103

### 104 **3. Methods**

105 X-ray diffraction analyses (XRD) were performed at the University of Lille and the  
106 LDEO (Lamont–Doherty Earth Observatory of Columbia University). In this paper, “clay  
107 minerals” refer to the major phyllosilicate minerals within the clay-size fraction (generally  
108 <2 mm). They are identified by XRD following the protocol of Holtzapffel (1985). All  
109 samples were first decalcified with 0.2 N HCl. The excess acid was removed by repeated  
110 washings with distilled water and centrifugations. The clay-size fraction was separated by  
111 settling according to Stokes’s law, concentrated by centrifugation, and oriented by wet  
112 smearing on glass slides. The analyses were run on a Philips PW 1749 generator (copper  
113 anode; 40 kV voltage; 25 mA intensity and 1°2 $\theta$ /min speed) at the University of Lille, and on  
114 a Philips X’Pert-MPD (q–q goniometer; Cu X-ray tube; Peltier-cooled, high sensitivity,  
115 Kevex energy dispersive detector) at the LDEO. A complete X-ray diffraction analysis  
116 requires several runs to permit precise mineral identification. Two XRD runs were performed  
117 routinely for each sample: (1) air-dried sample (“normal” run) and (2) ethylene-glycol  
118 vapour saturation for 12 h (“glycol” run). The analyses were run from 2.49° to 32.49° 2 $\theta$ .  
119 Each clay mineral is characterized by its basal layer plus interlayer interval (d) as revealed by  
120 XRD analysis (Brown and Brindley, 1980). Smectite (“S”) is characterized by a peak at 14 Å  
121 on the normal run, which expands to 17 Å after saturation by ethylene glycol. Illite (“I”)  
122 presents a basal peak at 10 Å on the two runs. Chlorite (“C”) is characterized by peaks at 14  
123 Å (001), 7 Å (002), 4.75 Å (003) and 3.53 Å (004) on the two diffraction spectra. Kaolinite  
124 (“K”) is characterized by peaks at 7 Å (001) and 3.58 Å (002) on the normal and glycol runs.  
125 To distinguish kaolinite from chlorite, the portion of the spectrum containing the basal peaks  
126 of kaolinite (002) and chlorite (004) around 3.55 Å is step-scanned in a high-resolution mode  
127 following standard procedures described in detail by Petschick et al. (1996). Semi-  
128 quantitative estimation of clay mineral abundances is based on peak areas, weighted by  
129 empirically estimated factors (Biscaye, 1965; Biscaye et al., 1997) and summed to 100% (S +  
130 I + K + C = 100%). Peak area measurements were realized in the glycol runs using the  
131 Macintosh Mac- Diff<sup>®</sup> 4.2.5 software (Petschick, 2000). Results are given in Tables 1 and 2.  
132 The error on the reproducibility of measurements is estimated to be  $\pm 5\%$  for each clay  
133 mineral. The mixed-layered clay minerals identified by Potter et al. (1975) in Ohio River and  
134 Tennessee River samples (sites 14 and 15) were not taken into account in the percentages  
135 since their exact nature (vermiculite and/or illite–chlorite and/or illite–smectite) is unknown.

136 All data were recalculated according to the  $S + I + K + C = 100\%$  formula in order to be  
137 compared to each other. The data have been gridded and contoured using the Surfer<sup>®</sup> 8  
138 software. For each clay mineral, scales between isolines of land and sea maps are different to  
139 allow a better representation of their relative variations in each environment. Map contours do  
140 not represent precise boundaries of clay mineral composition on land, but rather indicate  
141 rough limits between the dominant source areas of each clay mineral over the United States,  
142 based on our dataset.

143

#### 144 **4. Clay mineral distribution**

145 In most continental environments, illite and chlorite are usually inherited from ancient  
146 rocks (Palaeozoic, pre-Cambrian) modified by physical or moderate chemical weathering at  
147 high latitudes or altitude where Quaternary periglacial climatic conditions prevail. In North  
148 America, kaolinite forms through long-term weathering processes during preglacial time  
149 (Thiry et al., 1999; Thiry, 2000). It can derive from saprolites as well as from old sedimentary  
150 formations and may also form in solfatares in association with smectite (Huertas et al., 1999).  
151 Smectite is either derived from volcanic ash layers or authigenic in poorly-drained  
152 environments as in alluvial or coastal plains (Kraus, 1999; synthesis in Gerrard et al., 2007).  
153 Smectite can also be locally formed in the marine environment through early diagenesis,  
154 halmyrolysis (Karpoff et al., 1989), or hydrothermal weathering of volcanic rocks (Chamley,  
155 1998).

156

##### 157 *4.1. Clay mineral distributions in and around the Mississippi River watershed*

158 Three large areas can be distinguished based on smectite abundance patterns (Fig. 6a).  
159 The first covers a huge part of the Mississippi River watershed, including the Missouri River  
160 basin and Mississippi River alluvial plains. A corridor of high smectite values (>40%)  
161 extends from Saskatchewan to the Mississippi River mouth and separates two areas of low  
162 smectite content (<20%): the eastern Mississippi River and the north-western Texas  
163 watersheds. Smectite decreases rapidly (from 45% to 0% in few hundreds of kilometres) from  
164 the Mississippi River toward the eastern part of the United States of America (USA).

165 Due to the calculation method used, clay mineral percentages are not independent of  
166 each other. Because clay minerals are summed to 100%, variations in the two most abundant  
167 ones (smectite and illite) have opposite trends. Two major zones characterized by high illite  
168 concentrations can be observed in the distribution pattern of that mineral (Fig. 6b). Sediments  
169 exposed near the Great Lakes area are characterized by illite values >40%, especially the

170 areas northeast and southwest of Lake Huron. Similarly the clay mineral fraction of sediments  
171 from north-western Texas (Gulf Coast Rivers of the south-western USA and southwestern  
172 Mississippi River watersheds) contain more than 40% illite. Those two zones are separated by  
173 an illite depletion extending from the north-western Mississippi River basin to the south-  
174 eastern USA. This zone is composed of three minimal areas (<15%): Saskatchewan, the lower  
175 Arkansas River and Alabama-Florida coastal plains between the Mobile Embayment and the  
176 Apalachicola River mouth.

177 The south-eastern USA where soils and sediments are very rich in kaolinite (>30%) is  
178 one of the most important sources of this mineral. Kaolinite proportions are maximal in north  
179 Florida, exceeding 60% (Fig. 7a). Two other potential source areas for kaolinite, characterized  
180 by values around 20%, are located in the upper Mississippi River and around the Pecos River  
181 in Texas. The Missouri River system and the middle and lower Mississippi River alluvial  
182 plain sediments display low kaolinite content, contrasting with the high values to the west and  
183 to the east.

184 The chlorite distribution displays an East-West decreasing gradient (Fig. 7b). High  
185 values of chlorite (>20%) are found in the eastern part of the USA (east of about 087° W).  
186 Chlorite abundance decreases westward, first sharply down to about 10%, in the Mississippi  
187 River valley, and then more gradually, down to <4%, toward the Gulf of Mexico coastal  
188 plains, the western Mississippi River watershed and north-western Texas.

189 Since in most continental environments, smectite and kaolinite are generally formed  
190 by chemical weathering, while illite and chlorite are mostly inherited from ancient rocks  
191 modified by physical or moderate chemical weathering, the clay mineral ratio  
192  $(\text{smectite} + \text{kaolinite})/(\text{illite} + \text{chlorite})$  indicates the type of weathering (chemical or physical)  
193 that affected the erodible sediments. According to the distribution of this  $(S + K)/(I + C)$  ratio  
194 (Fig. 8), the North American continent east of the Rockies can be divided in different  
195 dominant weathering-regime areas.

196 The south-eastern United States is characterized by maximum values of the ratio (>4),  
197 suggesting that chemical weathering prevails in this region. This seems to be in agreement  
198 with the presence of yellow-red subtropical soils (Fig. 5). The important hydrolysis results  
199 from both high precipitation (>1000 mm/year) and high temperatures (>5 °C in winter and  
200 >25 °C in summer) that characterize this region. The north-eastern United States as well as  
201 the south-western Mississippi River watershed display minimum values of the  $(S + K)/(I + C)$   
202 ratio (<1). As expected from local climatic conditions and altitude, these areas seem to be  
203 dominated by physical weathering processes. The respective contributions of both physical

204 and chemical weathering can not be easily deduced in the other areas characterized by  
205 intermediate values of the  $(S + K)/(I + C)$  ratio.

206

#### 207 *4.2. Distribution in the northern Gulf of Mexico*

208 The clay mineral distribution maps of the Gulf of Mexico cover various  
209 geomorphologic provinces including the Texas slope, the Louisiana shelf and continental  
210 slope, the Mississippi River delta, the Alabama shelf, the Florida shelf and the deep-sea plain  
211 (Figs. 3, 6 and 7).

212 Smectite is the dominant clay mineral and represents more than 50% of the clay  
213 mineral fraction in surface sediments from the central and western parts of the Northern Gulf  
214 of Mexico (Table 1, Fig. 6a). The smectite content is lower on the Alabama and Florida  
215 shelves with values below 40%. The illite content ranges between 13% and 40% (Fig. 6b).  
216 Overall, the illite abundance decreases from the northern Gulf of Mexico continental shelves  
217 toward the deep-sea plain. This decreasing trend is particularly clear from the proximal to the  
218 distal parts of the Mississippi River Delta. Nevertheless, an illite-rich area extends from the  
219 Louisiana coasts to the deep-sea plain and constitutes an exception in the illite general trend.  
220 The distribution of kaolinite displays an overall West–East increasing gradient in the Gulf of  
221 Mexico (Fig. 7a). Kaolinite percentages are minimal (<20%) on the central and western parts  
222 of the northern Gulf of Mexico. They increase eastward and reach their maximum (>24%) on  
223 the Florida shelf. Chlorite is the least abundant clay mineral in the Gulf of Mexico, ranging  
224 from 0% to 20% (Fig. 6b). The chlorite content is minimal in the areas located off the  
225 Mississippi River mouth and in the Louisiana shelf (<4%), and maximum in the eastern and  
226 southern parts of the Northern Gulf of Mexico.

227

### 228 **5. Main clay mineral provinces of the United States of America east of the Rocky** 229 **Mountains**

230 The United States east of the Rockies can be subdivided in four major mineralogical  
231 provinces (Fig. 9) based on the distribution maps of the main clay minerals (Fig. 6 and 7).

232 (Zone 1) The western part of the Mississippi River watershed including the entire  
233 Missouri River system, is defined by high smectite content (>40%; Fig. 6a). The relative  
234 abundance of smectite reflects the mineralogy of the Great Plains soils (Allen et al., 1972;  
235 Smith, 2003). Early studies (Murray and Leininger, 1956; Pinsak and Murray, 1960) noticed  
236 that the Missouri River carries large amounts of smectite of bentonitic origin. Smectite in the  
237 north-western Mississippi river watershed could be related to aeolian volcanic deposits in

238 Canadian prairie soils (Curtin et al., 1998). Part of the smectite may also be authigenic and  
239 form in poorly drained soils, from the main Mississippi River valley or from the surrounding  
240 periglacial loess (Fig. 5; Pye and Johnson, 1988). Illite is less abundant, ranging from 10% to  
241 30% (Fig. 6b). In this province, an increase of illite in the detrital loads of rivers is observed  
242 after winter, when illite, formed through glaciogenic processes, by physical weathering and  
243 erosion of parent rocks, is easily removed by rainfall/meltwater and then exported towards the  
244 ocean via rivers (Weaver, 1967). The eastern part of this area (Wisconsin), in the Upper  
245 Mississippi River catchment basin between Lakes Superior and Michigan is characterized by  
246 locally higher kaolinite content (>20%; Fig. 7a). Kaolinite is derived commonly from a  
247 saprolite developed during the Mesozoic and early Tertiary on Precambrian basement,  
248 particularly in the area of River Falls (site 8 in Fig. 4; Irving, 1876; Cummings and Scrivner,  
249 1980).

250 (Zone 2) The region composed by the Great Lakes area and the eastern Mississippi  
251 River watershed is characterized mainly by illite (>25%; Fig. 6b) and chlorite-rich sediments  
252 (>20%; Fig. 7b). These minerals result from primarily physical weathering of lower/ middle  
253 Palaeozoic rocks (Appalachian Mountains; Griffin et al., 1968; Potter et al., 1975). This  
254 distribution pattern agrees with previous observations in the same area (Pinsak and Murray,  
255 1960; Weaver, 1967; Johnson and Kelley, 1984).

256 (Zone 3) The south-eastern United States region is typified by the relative abundance  
257 of kaolinite, often exceeding 40% (Fig. 7a). The erosion of Neogene marine terraces along the  
258 Georgia coast, which is covered by red-yellow podzolic soils, derived from the Appalachian  
259 Mountain saprolites (Fig. 5), yields kaolinite-rich sediments (Pirkle, 1960). The reflectance  
260 data of Balsam and Beeson (2003) support the hypothesis that Georgia is one of the main  
261 sources of kaolinite delivered to the Gulf of Mexico. The abundance of kaolinite in this  
262 province reflects mostly the composition of polygenetic palaeosoils, although produced at a  
263 lower rate today.

264 (Zone 4) The last province covers the south-western Mississippi River- and the Brazos  
265 River watersheds (Fig. 9). River clay loads from this area are mainly composed of illite  
266 (>50%; Fig. 6b) and kaolinite (>25%; Fig. 7a). High values of illite in this area are explained  
267 by the proximity of Colorado Plateau where frost shattering and other mechanical erosion  
268 processes reactivate recurrently in wintertime. The Llano Estacado, which is in the middle of  
269 this area (Fig. 5), is uplifted plateau of Late Tertiary riverine illite and kaolinite-rich sediments  
270 (Parry and Reeves, 1968; Glass et al., 1973; USGS Geological map).

271

272 **6. River inputs into the Gulf of Mexico and oceanographic implications**

273 Three processes largely control the distribution of continentally derived clay minerals  
274 in the sediments of the Northern Gulf of Mexico.

275

276 *6.1. River inputs*

277 According to Pinsak and Murray (1960), the main factor controlling the marine  
278 distribution of clay minerals is the nature of the dominant particle sources. Our data show that  
279 the Northern Gulf of Mexico can be roughly divided into two separated provinces: a western  
280 smectite-rich (>50%) and kaolinite-poor (<20%) province and (2) an eastern smectite-poor  
281 and kaolinite-rich province (Figs. 6a and 7a). This pattern clearly suggests that the clay  
282 mineral distribution in the Northern Gulf of Mexico is controlled by two main river systems.

283 The western smectite-rich province covers the main part of the Gulf of Mexico. This  
284 peculiar distribution reflects the prevailing detrital supply via the Mississippi River since the  
285 latter delivers the sediments to the Gulf of Mexico that are the most enriched in smectite (60–  
286 80%). This is consistent with the fact that Mississippi River discharge is 20 times larger than  
287 all other rivers combined feeding the Gulf of Mexico (Griffin, 1962; Chamley and Kennett,  
288 1976). As a consequence the fine-grained sedimentation in the Northern Gulf of Mexico is  
289 mainly controlled by the detrital inputs from the Mississippi River. Since the Mississippi  
290 River detrital supply is depleted in chlorite, the area directly under the influence of the  
291 Mississippi River inputs is characterized by chlorite-poor deposits (<4%; Fig. 7b).

292 The eastern kaolinite-rich province corresponds mainly to the Alabama–Florida shelf  
293 and the clay mineral assemblages probably signal a local origin. The Apalachicola River and  
294 the Mobile River system, which drain both the kaolinite-rich south-eastern continental  
295 province (Zone 3) and the chlorite-rich Appalachian Mountains (Zone 2; Fig. 9), likely  
296 account for the kaolinite- and chlorite-rich sediments onto this eastern province (Fig. 7).  
297 Parker et al. (1992) noted indeed that the provenance of the clay-mineral suite observed in the  
298 Alabama shelf is primarily from the Mobile River system. Moreover, Mazzullo and Peterson,  
299 1989 analysed the late Quaternary silts on the Northern Gulf of Mexico continental shelf and  
300 identified two provinces in the Alabama–Florida shelf which correspond to areas directly  
301 influenced by the Mobile River and Apalachicola River respectively. The coeval occurrence  
302 of high kaolinite and chlorite contents in surface sediments of the eastern province of the Gulf  
303 of Mexico is somehow surprising. Indeed, chlorite is early removed under the weathering  
304 conditions that prevail in Alabama, Florida and Cuba whereas kaolinite is likely to be more  
305 resistant. Such characteristics suggest that chlorite and kaolinite must result from at least two

306 different source rivers (as reflected by different stages of weathering). Unfortunately we have  
307 not found data to support this hypothesis yet. Russell et al. (2000) noticed that chlorite is one  
308 alteration mineral in the Encrucijada Formation, of Albian–Cenomanian age, west of Havana.  
309 This chlorite may be currently (or have been over the recent past) transported to the Gulf of  
310 Mexico and may explain the high chlorite content in sediment off Cuba.

311 Balsam and Beeson (2003) delineated transport and dispersal paths for kaolinite based  
312 on the factor analysis of the first derivatives of the percent reflectance data from 186 core-top  
313 and grab samples distributed throughout the Gulf of Mexico. They proposed that kaolinite  
314 from the Mobile River system is transported across the shelf and into deeper portions of the  
315 Gulf. This is in agreement with our observations and may explain why sediments off Mobile  
316 Bay and of the Mississippi River Delta have slightly higher kaolinite content (>12%) than  
317 sediments of the Louisiana continental slope (Fig. 7a).

318 The other northern Gulf-Coast Rivers (e.g. Atchafalaya, Brazos, and Rio Grande  
319 rivers) have more local influences. Atchafalaya Bay delivers illite-rich sediments to the  
320 Louisiana shelf. These sediments are further transported across the Louisiana slope and into  
321 the deep Gulf of Mexico (Fig. 6b). The Rio Grande and/or its tributary (the Pecos River) drain  
322 the illite- and kaolinite-rich continental province defined as Zone 4 (Fig. 9) and distribute  
323 illite-rich sediments (>26%) over the Texas continental shelf and slope (Fig. 6b). Similarly,  
324 the clay mineral fraction of sediments off the Rio Grande and into the deep-sea plain are  
325 richer in kaolinite than Louisiana continental slope deposits, in agreement with Balsam and  
326 Beeson (2003) results. However, the respective kaolinite concentration maps show some  
327 discrepancies. According to Balsam and Beeson results (2003), the maximum kaolinite  
328 concentration area is located in the deep-sea plain of the Gulf of Mexico. Kaolinite content is  
329 highest in sediments of the Alabama–Florida shelf in our distribution map, in agreement with  
330 the previous work of Griffin (1962). Moreover, the comparison of kaolinite distribution map  
331 on the continent with marine distribution map suggests a clear relationship between the major  
332 continental source of kaolinite and the kaolinite-rich Alabama–Florida shelves (Zone 3; Fig.  
333 9).

334

### 335 *6.2. Differential settling*

336 A regular offshore decrease of illite contents off the main Northern Gulf-coast Rivers  
337 with an exception for the Atchafalaya Bay appears on the illite distribution map (Fig. 6b).  
338 Illite generally has the largest grain size distribution of the clay mineral fraction in the  
339 Mississippi River suspended sediment (Johnson and Kelley, 1984; their figure 2) and in loess.

340 Even when illite floccules are smaller than those of smectite, they are denser (Sakamoto,  
341 1972), and consequently, illite settles more rapidly than the other clay minerals. The observed  
342 zoned pattern suggest that differential settling, with larger flocs and grain-size being  
343 deposited nearest shore, is one of the processes affecting clay mineral distribution in the  
344 Northern Gulf of Mexico. The distributions of various clay mineral peak-area ratios  
345 (illite/smectite, illite/kaolinite, illite/chlorite [maps not shown]) over the Northern Gulf of  
346 Mexico confirm the apparent decrease in abundance of illite towards the deeper basin. This  
347 local differential settling of clay minerals has not been previously reported elsewhere in Gulf  
348 of Mexico sediments (Pinsak and Murray, 1960; Griffin, 1962; Scafe and Kunze, 1971; Doyle  
349 and Sparks, 1980).

350

### 351 **6.3. Oceanic processes**

352 In addition to river inputs and differential settling, oceanic currents may also affect the  
353 distribution of clay minerals in the Northern Gulf of Mexico sediments. The surface  
354 circulation over the Gulf of Mexico, especially along the coast is modulated seasonally by  
355 changes in primary wind patterns. The dominant hydrologic feature of the Gulf of Mexico is  
356 the clockwise Loop Current (Fig. 1). The Loop Current enters the Gulf through the Yucatan  
357 Channel, intrudes variably northward, sometimes as far as the Mississippi Delta, and exits  
358 through the Florida Straits. Anti-cyclonic rings (Loop Current Rings) separate from the Loop  
359 Current every 6–17 months and travel westward across the Gulf of Mexico (Ohlmann and  
360 Niiler, 2005). General circulation on the Louisiana– Texas shelf is dominated by a cyclonic  
361 gyre, resulting in a strong, westward, coastal current associated with a relatively weak  
362 eastward current along the shelf break.

363 These hydrological features most likely influence the marine clay mineral distribution  
364 patterns in the Gulf of Mexico (Figs. 6 and 7). The geographical extent of the two distinct  
365 clay mineral marine provinces (see Section 6.1) is indeed consistent with an anti-cyclonic  
366 transport in the north-eastern Gulf of Mexico driven in part by the Loop Current. For instance,  
367 an eastward transportation of Mississippi sediments enriched in smectite is apparent on the  
368 western Alabama shelf. Similarly, southward transportation of the Apalachicola River  
369 kaolinite-rich sedimentary load clearly occurs over the Florida shelf (Figs. 1, 6a and 7a).

370 In the western part of the Gulf of Mexico, the chlorite-poor Louisiana continental shelf  
371 deposits likely result from a westward transportation of the Mississippi River chlorite-poor  
372 sedimentary load due to the dominant oceanic currents that affect this area (Fig. 7b). This  
373 transport pattern is not clear in the smectite distribution map due to its lower resolution (i.e.

374 higher range of values). Likewise, the illite-rich suspended sediments from the Rio Grande  
375 River are transported eastward over the Texas continental slope under the influence of the  
376 prevailing eastward oceanic currents.

377 The overall distribution of clay mineral assemblages in the Gulf of Mexico is in  
378 agreement with previously proposed sediment dispersal paths in the area excepted for the  
379 Florida shelf (Balsam and Beeson, 2003; Ellwood et al., 2006).

380

## 381 **7. Conclusions**

382 Clay mineral distribution maps of the North American continent and over the Northern  
383 Gulf of Mexico were generated using clay mineral data from erodible/alluvial sediments on  
384 land and from marine surface sediments. The United States can be divided into four provinces  
385 representing the main clay mineral source areas for sediments exported toward the Gulf of  
386 Mexico. The north-western Mississippi River watershed is characterized by high smectite  
387 content which reflects both the composition of Cretaceous, Tertiary and Pleistocene bedrock  
388 associated with a bentonitic or authigenic origin. The Great Lakes area and the Ohio–  
389 Tennessee River catchment areas deliver mainly illite and chlorite, due to the chiefly physical,  
390 as opposed to chemical, weathering and erosion of Palaeozoic rocks. The Brazos River and  
391 south-western Mississippi River watersheds are dominated by illite and kaolinite released by  
392 the erosion of the Colorado Plateau and the Llano Estacado. The south-eastern part of the  
393 United States constitutes a major kaolinitic province. This kaolinite is derived from inherited  
394 red yellow podzolic soils.

395 The comparison of clay distribution patterns of marine surface sediments with results  
396 obtained on the continent permits the identification of three main factors controlling clay-  
397 mineral distribution in the Gulf of Mexico. (1) Relative fluvial contribution is the most  
398 important factor controlling the clay mineral composition of marine sediments. The dominant  
399 source is the terrigenous supply via the Mississippi River as supported by the high smectite  
400 content over the Northern Gulf of Mexico, whereas the Mobile, Apalachicola, Atchafalaya,  
401 Rio Grande and Brazos Rivers inputs have more local influences. (2) Differential settling,  
402 suggested by the illite gradient from the coast to the deep sea off the main Gulf- Coast Rivers,  
403 is identified as a contributing factor controlling clay distribution locally in the Gulf of  
404 Mexico. (3) Surface oceanic currents, controlled by either the Loop Current or seasonal  
405 winds, influence the distribution of clay minerals. We can identify a southward transport of  
406 the Mobile and Apalachicola kaolinite-rich sediments over the Florida shelf; a westward  
407 transport of Mississippi-derived, chlorite-poor river sediments due to westward currents

408 affecting the eastern part of the Louisiana shelf and an eastward transport of Rio Grande  
409 suspended sediments over the Texas slope. The distribution of the two clay mineral marine  
410 provinces (the western smectite-rich province and the eastern kaolinite-rich province) is  
411 indeed coherent with the anti-cyclonic north-eastern Gulf of Mexico circulation influenced by  
412 the Loop Current. This overview of the dominant factors controlling recent clay mineral  
413 distributions in the Gulf of Mexico within the studied transect lays the groundwork for the use  
414 of clay-mineral assemblages for downcore investigations, particularly during the last glacial  
415 cycle when clay mineral fluvial inputs have likely been different from those of today due to  
416 the presence of the Laurentide Ice Sheet which modified the erosional pattern. The study of  
417 the clay mineral assemblages supplied to the Gulf of Mexico during meltwater pulses should,  
418 for instance, provide valuable information on their provenance, and therefore contribute to  
419 documenting the climatic conditions over the North American continent during the last glacial  
420 period (Sionneau et al., in preparation).

421

#### 422 **Acknowledgements**

423 The authors would like to thank Bruno Minguely for his assistance on the Surfer software.  
424 We gratefully acknowledge Yvon Balut, the Institut Polaire Français Paul-Emile Victor, the  
425 officers and crew of the Marion Dufresne and the IMAGES program for marine sediment core  
426 collection. This work was supported by the “Géosystèmes” Laboratory of the University of  
427 Lille 1 (France) and by the Lamont–Doherty Earth Observatory of Columbia University  
428 (USA). The authors thank William L. Balsam and an anonymous reviewer for their helpful  
429 and constructive comments on the manuscript. This is LDEO Contribution No. 7181.

430

#### 431 **References**

- 432 Aharon, P., 2003. Meltwater flooding events in the Gulf of Mexico revisited: Implications for  
433 rapid climate changes during the last deglaciation. *Paleoceanography* 18, 1079.  
434 doi:10.1029/2002PA000840.
- 435 Allen, B.L., Harris, B.L., Davis, K.R., Miller, G.B., 1972. The mineralogy and chemistry of  
436 high plains playa lake soils and sediments. Report WRC 72-4, Texas Tech. University, 75 pp.
- 437 Balsam, W.L., Beeson, J.P., 2003. Sea-floor sediment distribution in the Gulf of Mexico.  
438 *Deep-Sea Research* 50, 1421–1444.
- 439 Biscaye, P.E., 1965. Mineralogy and sedimentation of recent deep-sea clay in the Atlantic  
440 Ocean and adjacent seas and oceans. *GSA Bulletin* 76, 803–832.
- 441 Biscaye, P.E., Eittrheim, S., 1977. Suspended particulate loads and transports in the nepheloid

442 layer of the abyssal Atlantic Ocean. *Marine Geology* 23, 155–172.

443 Biscaye, P.E., Grousset, F.E., Revel, M., Van der Gaast, S., Zielinski, G.A., Vaars, A., Kukla,  
444 G., 1997. Asian provenance of glacial dust (stage 2) in the Greenland Ice Sheet Project 2 Ice  
445 Core, Summit, Greenland. *Journal of Geophysical Research* 102, 26,765–26,781.

446 Bond, G.C., 1995. Climate and the conveyor. *Nature* 377, 383–384.

447 Boulay, S., Colin, C., Trentesaux, A., Frank, N., Liu, Z., 2005. Sediment sources and East  
448 Asian monsoon intensity over the last 450 ky. Mineralogical and geochemical investigations  
449 on South China Sea sediments. *Paleogeography, Paleoclimatology, Paleoecology* 228, 260–  
450 277.

451 Bout-Roumazeilles, V., Trentesaux, T., 2006. Sedimentologic analysis of cores recovered  
452 from the Marion Dufresne cruise in the Gulf of Mexico, 2–18 July 2002. In: Winters, W.,  
453 Lorenson, T.D., Paull, C.K. (Eds.), Initial Report of the IMAGES VIII/PAGE 127 Gas  
454 Hydrate and Paleoclimate Cruise on the Marion Dufresne in the Gulf of Mexico, p. 29. 2–18  
455 July 2002, US Geological Survey, Open-File Report 2004-1358.

456 Broecker, W.S., 1991. The great ocean conveyor. *Oceanography* 4, 79–89.

457 Broecker, W.S., Kennett, J.P., Flower, B.P., Teller, J.T., Trumbore, S., Bonani, G., Wolfli,  
458 W., 1989. Routing of meltwater from the Laurentide Ice Sheet during the Younger Dryas cold  
459 episode. *Nature* 341, 318–321.

460 Broecker, W.S., Bond, G., Klas, M., Bonani, G., Wolfli, W., 1990. A salt oscillator in the  
461 glacial Atlantic? 1. The concept. *Paleoceanography* 5 (4), 469–477.

462 Brown, A.V., Brown, K.B., Jackson, D.C., Pierson, W.K., 2005. Lower Mississippi River and  
463 its tributaries. In: Benke, A.C., Cushing, C.E. (Eds.), *Rivers of North America*. Elsevier  
464 Academic Press, London, pp. 231–271.

465 Brown, G., Brindley, G.W., 1980. X-ray diffraction procedures for clay mineral  
466 identification. In: Brindley, G.W., Brown, G. (Eds.), *Crystal Structures of Clay Minerals and  
467 their X-ray Identification*. Mineralogical Society, London, pp. 305–359.

468 Brown, P.A., Kennett, J.P., 1998. Megaflood erosion and meltwater plumbing changes during  
469 the last North American deglaciation recorded in Gulf of Mexico sediments. *Geology* 26,  
470 599–602.

471 Chamley, H., 1998. Clay mineral sedimentation in the ocean. In: Paquet, H., Clauer, N.  
472 (Eds.), *Soils and Sediments (Mineralogy and Geochemistry)*. Springer, Berlin, pp. 269–302.

473 Chamley, H., 1989. *Clay Sedimentology*. Springer, Berlin, 623 pp.

474 Chamley, H., Kennett, J.P., 1976. Argiles détritiques, Foraminifères planctoniques et  
475 paléoclimats, dans des sédiments quaternaires du golfe du Mexique. *C.R. Acad. Sci. Paris*

476 282, 1415–1418.

477 Clark, P.U., Marshall, S.J., Clarke, G.K.C., Hostetler, S.W., Licciardi, J.M., Teller, J.T., 2001.  
478 Freshwater forcing of abrupt climate change during the last glaciation. *Science* 293, 283–287.

479 Clarke, G.K.C., Leverington, D.W., Teller, J.T., Dyke, A.S., 2003. Superlakes, megafloods,  
480 and abrupt climate change. *Science* 301, 922–923.

481 Cummings, M.L., Scrivner, J.V., 1980. The saprolite at the precambrian–cambrian contact,  
482 Irvine Park, Chippewa Falls, Wisconsin. *Transactions of the Wisconsin Academy of Sciences.*  
483 *Arts and Letters* 68, 22–29.

484 Curtin, D., Selles, F., Steppuhn, H., 1998. Estimating calcium-magnesium selectivity in  
485 smectitic soils from organic matter and texture. *Soil Science Society of America Journal* 62  
486 (5), 1280–1285.

487 Dahm, C.N., Edwards, R.J., Gelwick, F.P., 2005. Gulf Coast Rivers of the southwestern  
488 United States. In: Benke, A.C., Cushing, C.E. (Eds.), *Rivers of North America*. Elsevier  
489 Academic Press, London, pp. 181–219.

490 Delong, M.D., 2005. Upper Mississippi River Basin. In: Benke, A.C., Cushing, C.E. (Eds.),  
491 *Rivers of North America*. Elsevier Academic Press, London, pp. 327–362.

492 Doyle, L.J., Sparks, T.N., 1980. Sediments of the Mississippi, Alabama, and Florida  
493 (MAFLA) Continental Shelf. *Journal of Sedimentary Petrology* 50, 905–916.

494 Ellwood, B.B., Balsam, W.L., Roberts, H.H., 2006. Gulf of Mexico sediment sources and  
495 sediment transport trends from magnetic susceptibility measurements of surface samples.  
496 *Marine Geology* 203, 237–248.

497 Fagel, N., Hillaire-Marcel, C., Robert, C., 1997. Changes in the Western Boundary  
498 Undercurrent outflow since the Last Glacial Maximum, from smectite/illite ratios in deep  
499 Labrador Sea sediments. *Paleoceanography* 12, 79–96.

500 Fan, S., Oey, L., Hamilton, P., 2004. Assimilation of drifter and satellite data in a model of  
501 the Northeastern Gulf of Mexico. *Continental Shelf Research* 24, 1001–1013.

502 Flower, B.P., Hastings, D.W., Hill, H.W., Quinn, T.M., 2004. Phasing of deglacial warming  
503 and Laurentide Ice Sheet meltwater in the Gulf of Mexico. *Geology* 32, 597–600.

504 Galat, D.L., Berry Jr., C.R., Peters, E.J., White, R.G., 2005. Missouri River Basin. In: Benke,  
505 A.C., Cushing, C.E. (Eds.), *Rivers of North America*. Elsevier Academic Press, London 727–  
506 468.

507 Gallet, S., Jahn, B.M., Van Vliet Lanoe, B., Dia, A., Rossello, E., 1998. Loess geochemistry  
508 and its implications for particle origin and composition of the upper continental crust. *Earth*  
509 *and Planetary Science Letters* 156, 157–172.

510 Gerrard, M., Caquineau, S., Pinheiro, J., Stoops, G., 2007. Weathering and allophone  
511 neoformation in soils developed on volcanic ash in the Azores. *European Journal of Soil*  
512 *Science* 58, 496–515.

513 Gingele, F.X., De Deckker, P., Hillenbrand, C.-D., 2001. Clay mineral distribution in surface  
514 sediments between Indonesia and NW Australia source and transport by ocean currents.  
515 *Marine Geology* 179, 135–146.

516 Glass, H.D., Frye, J.C., Leonard, A.B., 1973. Clay minerals in east-central New Mexico. New  
517 Mexico Bureau of Geology and Mineral Resources. Circular 139, 14.

518 Gradusov, B.P., 1974. A tentative study of clay mineral distribution in soils of the world.  
519 *Geoderma* 12, 49–55.

520 Griffin, G.M., 1962. Regional clay mineral facies. Products of weathering intensity and  
521 current distribution in the northeastern Gulf of Mexico. *Geological Society*  
522 *of America Bulletin* 73, 737–768.

523 Griffin, J.J., Goldberg, E.D., 1969. Recent sediments of Caribbean Sea. *The American*  
524 *Association of Petroleum Geologists* 11, 258–268.

525 Griffin, J.J., Windom, H., Goldberg, E.D., 1968. The distribution of clay minerals in the  
526 World Ocean. *Deep-Sea Research* 15, 433–459.

527 Haug, G.H., Tiedemann, R., 1998. Effect of the formation of the Isthmus of Panama on  
528 Atlantic Ocean thermohaline circulation. *Nature* 393, 673–676.

529 Holtzapffel, T., 1985. Les minéraux argileux: Préparation, Analyse Diffractométrique et  
530 Détermination. Société Géologique du Nord, Villeneuve d'Ascq, 136 pp.

531 Huertas, F.J., Fiore, S., Huertas, F., Linares, J., 1999. Experimental study of the hydrothermal  
532 formation of kaolinite. *Chemical Geology* 156, 171–190.

533 Irving, R.D., 1876. On Kaolin in Wisconsin. *Wisconsin Academy of Science Arts and Letters*  
534 *Transactions* 3, 3–30.

535 Johnson, A.G., Kelley, J.T., 1984. Temporal, spatial, and textural variation in the mineralogy  
536 of Mississippi River suspended sediment. *Journal of Sedimentary Petrology* 54, 67–72.

537 Jones, G.A., 1984. Advective transport of clay minerals in the region of the Rio Grande Rise.  
538 *Marine Geology* 58, 187–212.

539 Joyce, J.E., Tjalsma, L.R.C., Prutzman, J.M., 1993. North American glacial meltwater history  
540 for the past 2.3 m.y.: Oxygen isotope evidence from the Gulf of Mexico. *Geology* 21, 483–  
541 486.

542 Karpoff, A.M., Lagabriele, Y., Boillot, G., Girardeau, J., 1989. L'authigenèse océanique de  
543 palygorskite par halmyrolyse de péridotites serpentinisées (marge de Galice); ses implications

544 géodynamiques. Comptes Rendus de l'Académie des Sciences, Série 2, Mécanique, Physique,  
545 Chimie, Sciences de l'Univers. Sciences de la Terre 308, 647–654.

546 Kennett, J.P., Shackleton, N.J., 1975. Laurentide Ice Sheet Meltwater Recorded in Gulf of  
547 Mexico Deep-Sea Cores. *Science* 188, 147–150.

548 Kraus, M.J., 1999. Paleosols in clastic sedimentary rocks: their geologic applications. *Earth*  
549 *Science Reviews* 47, 41–70.

550 Laj, C., Labeyrie, L., Kissel, C., 2004. Le rapport de campagne à la mer MD 132/ PICASSO -  
551 IMAGES XI à bord du Marion Dufresne. OCE/2004/02.

552 Leventer, A., Williams, D.F., Kennett, J.P., 1982. Dynamics of the Laurentide ice sheet  
553 during the last deglaciation: evidence from the Gulf of Mexico. *Earth and Planetary Science*  
554 *Letters* 59, 11–17.

555 Manabe, S., Stouffer, R.J., 1997. Coupled ocean-atmosphere model response to freshwater  
556 input: Comparison to Younger Dryas event. *Paleoceanography* 12, 321–336.

557 Matthews, W.J., Vaughn, C.C., Gido, K.B., Marsh-Matthews, E., 2005. Southern Plains  
558 Rivers. In: Benke, A.C., Cushing, C.E. (Eds.), *Rivers of North America*. Elsevier Academic  
559 Press, London, pp. 283–314.

560 Mazzullo, J., Peterson, M., 1989. Sources and dispersal of late Quaternary silt on the northern  
561 Gulf of Mexico continental shelf. *Marine Geology* 86, 15–26.

562 Murray, H.H., Leininger, R.K., 1956. The effect of weathering on clay minerals. *Clays Clay*  
563 *Minerals. Proceedings of the National Conference on Clays and Clay Minerals* 4, 340–347.

564 Ohlmann, J.C., Niiler, P.P., 2005. Circulation over the continental shelf in the northern Gulf  
565 of Mexico. *Progress in Oceanography* 64, 45–81.

566 Parker, S.J., Shultz, A.W., Schroeder, W.W., 1992. Sediment characteristics and seafloor  
567 topography of a palimpsest shelf, Mississippi–Alabama continental shelf. *Quaternary Coasts*  
568 *of the United States: Marine and Lacustrine Systems SEPM Special Publication*, no. 48, ISBN  
569 0-918985-98-6.

570 Parry, W.T., Reeves, C.C., 1968. Clay mineralogy of pluvial lake sediments, southern High  
571 Plains, Texas. *Journal of Sedimentary Research* 38, 516–529.

572 Petschick, R. 2000. MacDiff 4.2 Manual. MacDiff [Online]. Available from: <<http://www.geologie.uni-frankfurt.de/Staff/Homepages/Petschick/RainerE.html>>. (Revised 2001-  
573 05-17)

574  
575 Petschick, R., Kuhn, G., Gingele, F., 1996. Clay mineral distribution in surface sediments of  
576 the South Atlantic: sources, transport, and relation to oceanography. *Marine Geology* 130,  
577 203–229.

578 Pinsak, A.P., Murray, H.H., 1960. Regional clay mineral patterns in the Gulf of Mexico.  
579 Clays and Clay Minerals, 7th National Conference, Pergamon, Oxford, New York, pp. 162-  
580 177.

581 Pirkle, E.C., 1960. Kaolinitic sediments in peninsular Florida and origin of the kaolin.  
582 Economic Geology 55, 1382–1405.

583 Potter, P.E., Heling, D., Shimp, N.E., van Wie, W., 1975. Clay mineralogy of modern alluvial  
584 muds of the Mississippi River Basin. Bulletin du Centre Recherche Pau- SNPA 9, 353–389.

585 Pye, K., Johnson, R., 1988. Stratigraphy, geochemistry, and thermoluminescence ages of  
586 lower. Mississippi Valley loess Earth Surface Processes and Landforms 13 (2), 103–124.

587 Rahmstorf, S., 1995. Bifurcations of the Atlantic thermohaline circulation in response to  
588 changes in the hydrological cycle. Nature 378, 145–149.

589 Rateev, M.A., Gorbunova, Z.N., Lisitzin, A.P., Nosov, G.I., 1969. The distribution of clay  
590 minerals in the oceans. Sedimentology 13, 21–43.

591 Russell, N., Moreira, J., Sanchez, R., 2000. Volcanogenic massive sulphide deposits of Cuba.  
592 VMS deposits of Latin America. Geological Association of Canada, 241–258, Mineral  
593 Deposits Division, Special Publications, no. 2 pp.

594 Sakamoto, W., 1972. Study on the process of river suspension from flocculation to  
595 accumulation in estuary. Bulletin of Ocean Research Institute, University of Tokyo 5, 1-49.

596 Scafe, D.W., Kunze, G.W., 1971. A clay mineral investigation of six cores from the Gulf of  
597 Mexico. Marine Geology 10, 69–85.

598 Schmitz, W.J. Jr., 2003. On the Circulation In and Around the Gulf of Mexico. Volume I: A  
599 Review of the Deep Water Circulation. Available from: <[http://www.serf.  
600 tamus.edu/gomcirculation/](http://www.serf.tamus.edu/gomcirculation/)>. (Revised 2005-10-26)

601 Smith, L.M., 2003. Playas of the Great Plains. University of Texas Press, 275 pp.

602 Smith, S.R., Jacobs, G.A., 2005. Seasonal circulation fields in the northern Gulf of Mexico  
603 calculated by assimilating current meter, shipboard ADCP, and drifter data simultaneously  
604 with the shallow water equations. Continental Shelf Research 25, 157–183.

605 Teller, J.T., 1995. History and drainage of large ice-dammed lakes along the Laurentide Ice  
606 Sheet. Quaternary International 28, 83–92.

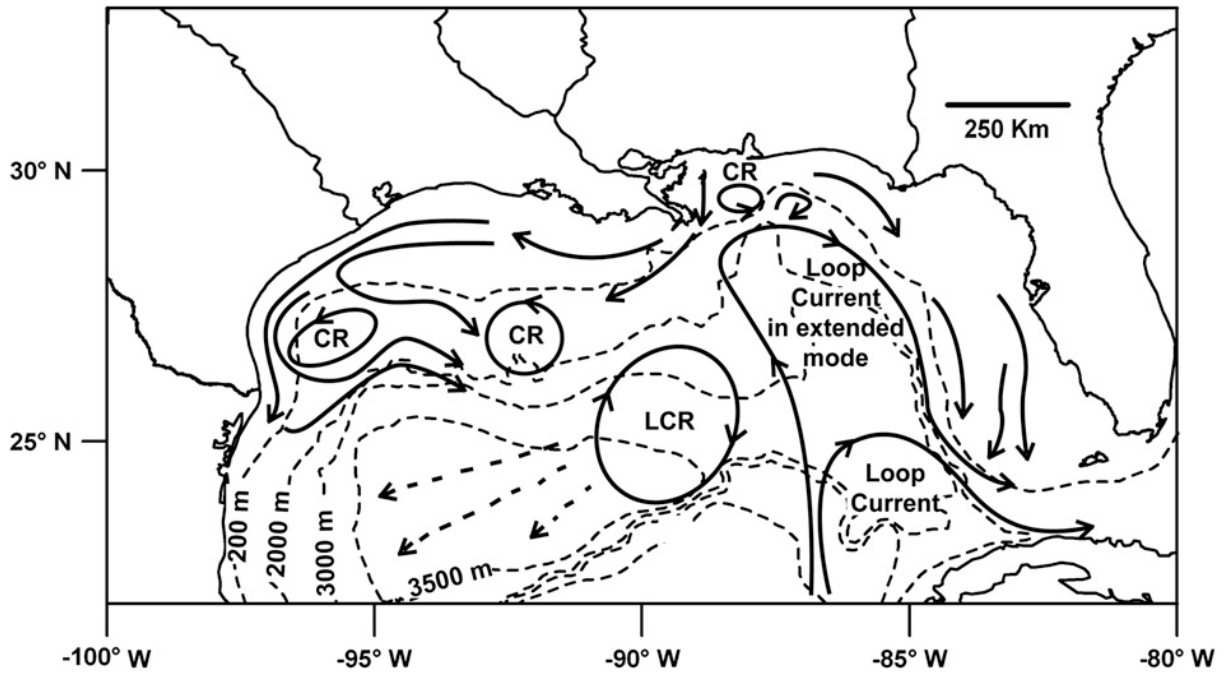
607 Thiry, M., 2000. Paleoclimatic interpretation of clay minerals in marine deposits: an outlook  
608 from the continental origin. Earth Science Review 49, 201–221.

609 Thiry, M., Simon-Coinçon, R., Schmitt, J.-M., 1999. Paléoaltérations kaoliniques:  
610 signification climatique et signature dans la colonne sédimentaire. C.R. Acad. Sci. Earth &  
611 Planetary Sciences 329, 853–863.

- 612 Vukovich, F.M., Crissman, B.W., 1986. Aspects of warm rings in the Gulf of Mexico. *Journal*  
613 *of Geophysical Research* 91, 2645–2660.
- 614 Weaver, C.E., 1967. Variability of a river clay suite. *Journal of Sedimentary Petrology* 37,  
615 971–974.
- 616 White, D., Johnston, K., Miller, M., 2005. Ohio River Basin. In: Benke, A.C., Cushing, C.E.  
617 (Eds.), *Rivers of North America*. Elsevier Academic Press, London, pp. 375–412.
- 618 Windom, H.L., 1976. Lithogenous material in marine sediments. In: Riley, J.P., Chester, R.  
619 (Eds.), *Chemical Oceanography*. Academic Press, New York, London, pp. 103–135.

620 **Figure captions**

621

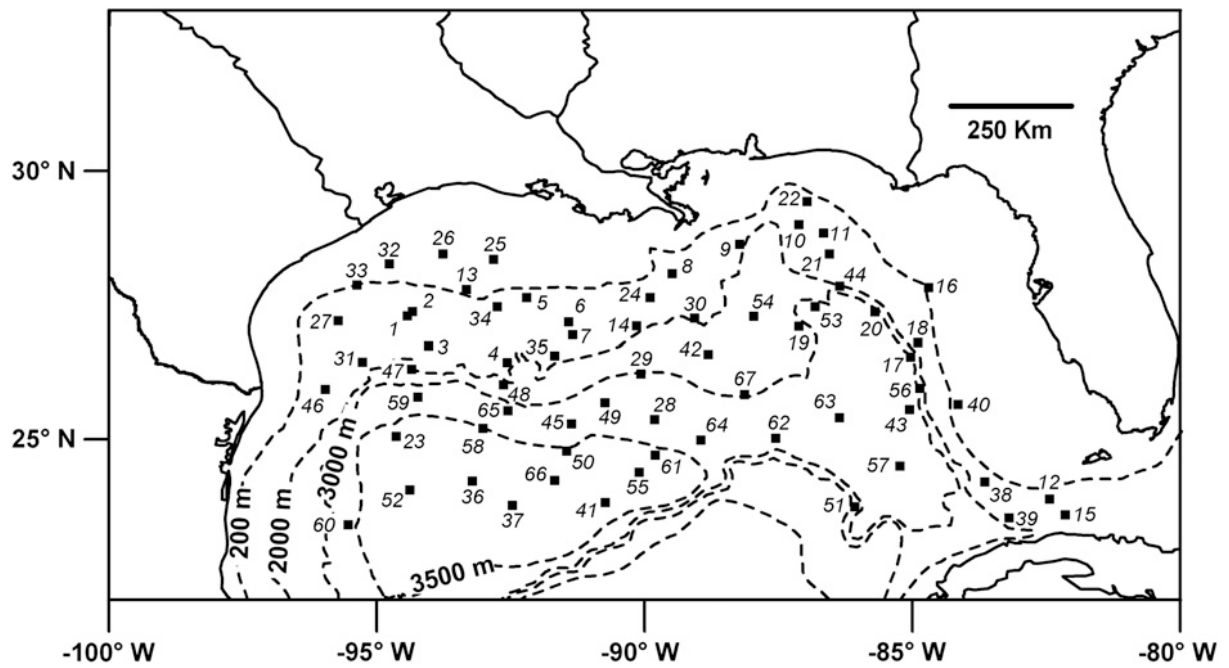


622

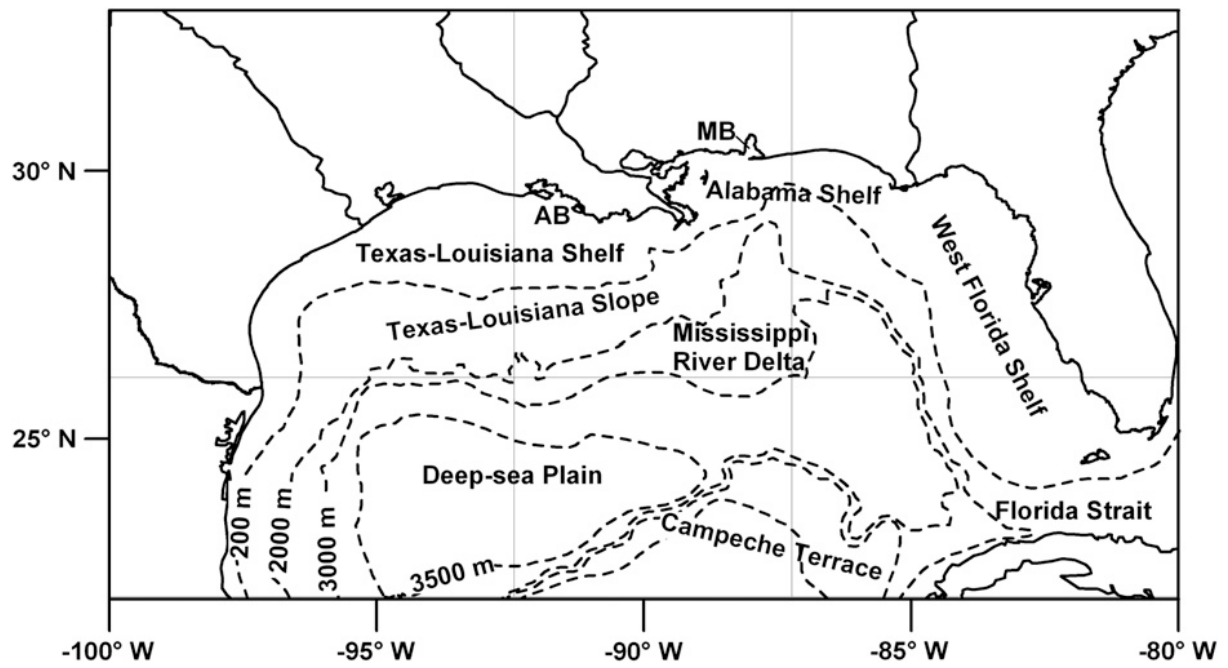
623 Fig. 1. Mean currents of the Gulf of Mexico (bold black arrows), including two different  
624 states of the Loop Current, Loop Current Rings (LCR) and Cyclonic Rings (CR) (adapted  
625 from Schmitz, 2003; Fan et al., 2004; Ohlmann and Niiler, 2005; Smith and Jacobs, 2005).

626 Dotted arrows represent propagation direction for LCR (Vukovich and Crissman, 1986).

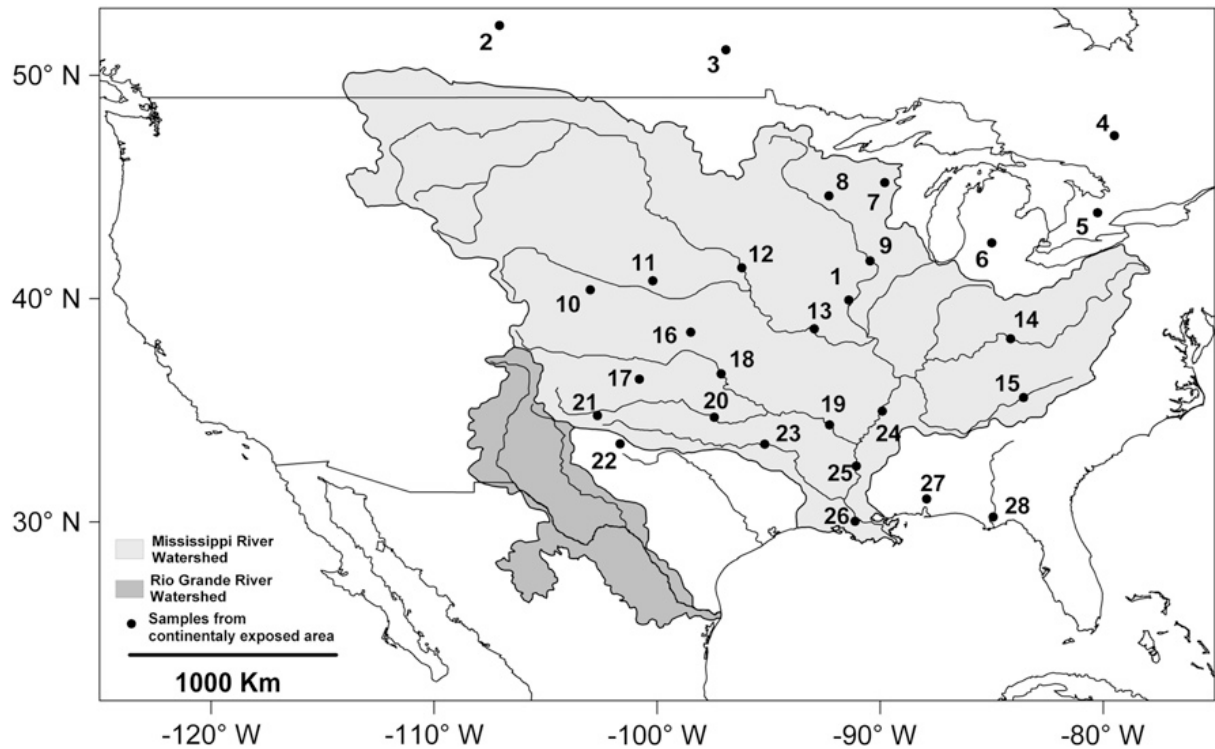
627



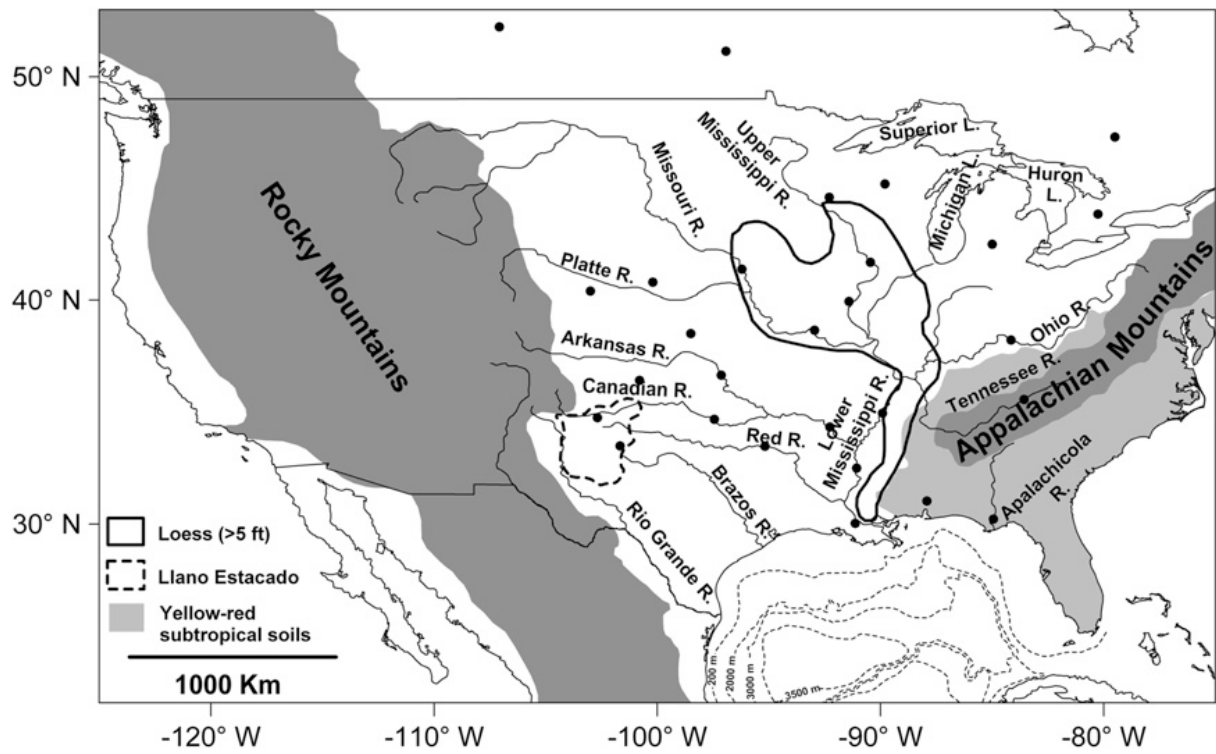
628  
 629 Fig. 2. Location of the 67 marine cores (1–67) recovered during RVs Robert Conrad, Vema,  
 630 Atlantis and Marion Dufresne cruises (RC, VM, AT and MD respectively in Table 1).  
 631



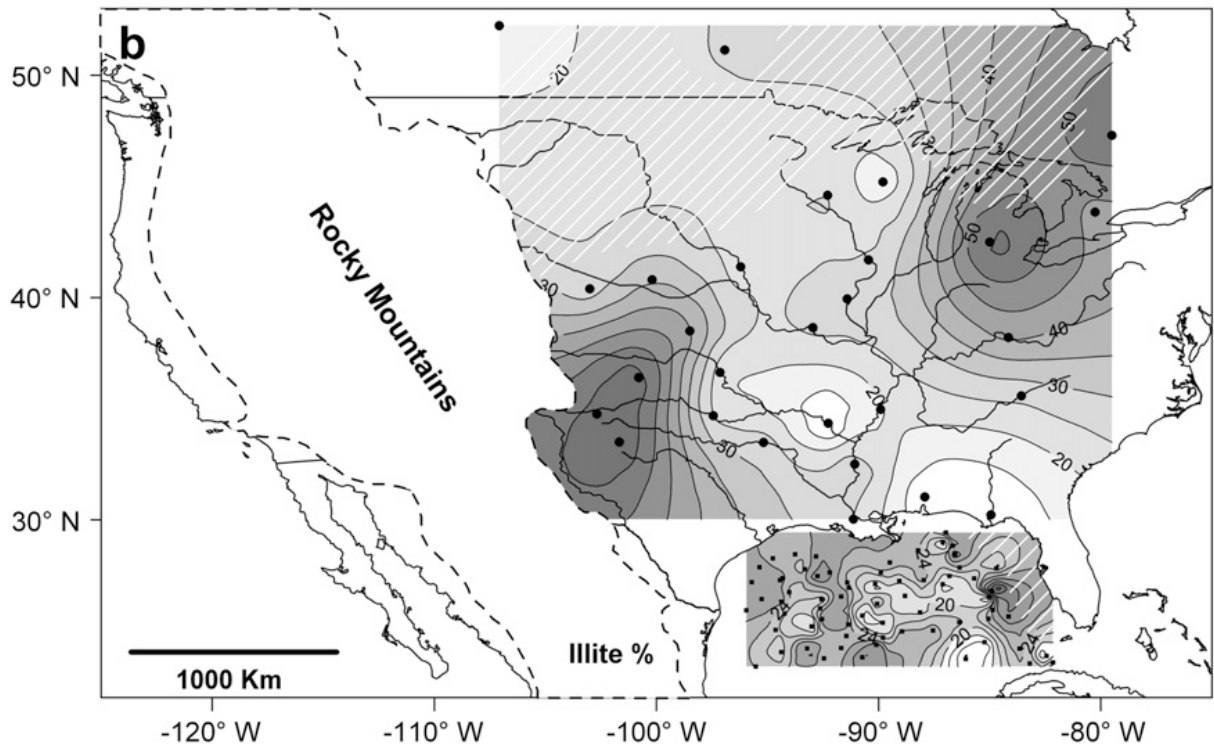
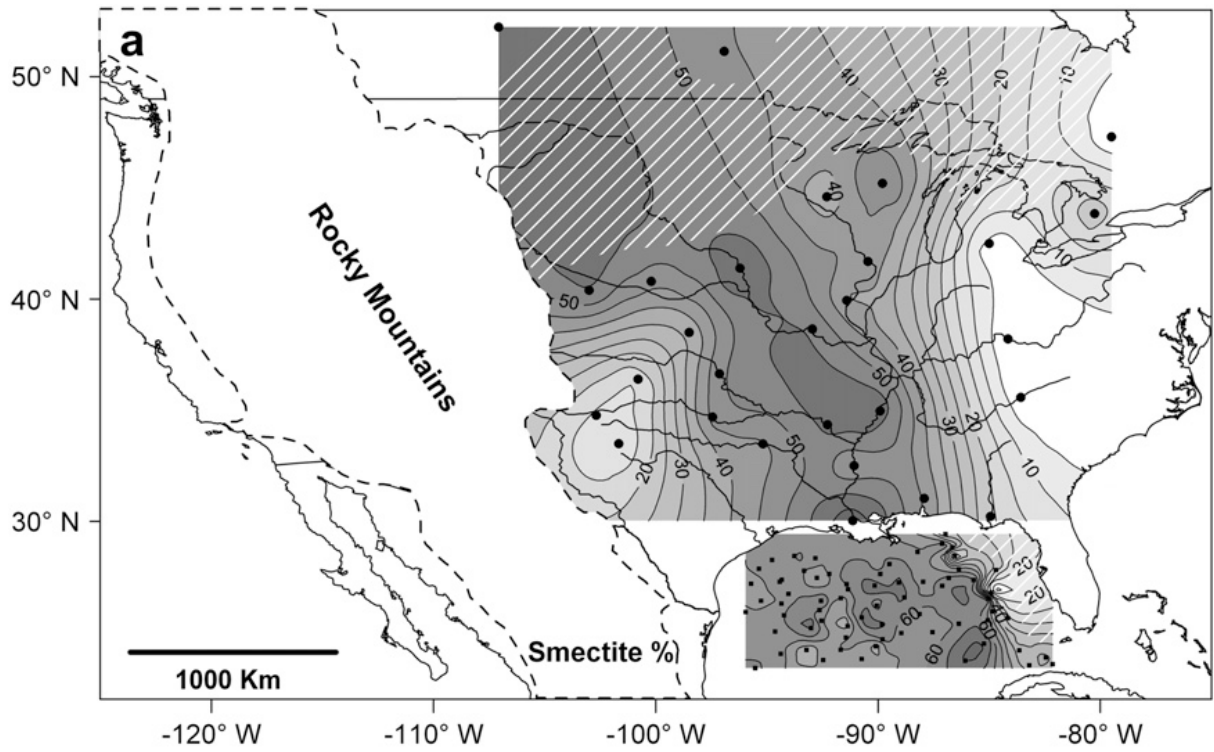
632  
 633 Fig. 3. Geomorphologic provinces of the Gulf of Mexico (AB: Atchafalaya Bay; MB: Mobile  
 634 Bay).



635  
 636 Fig. 4. Location of the 28 North American (1–28) sites used in the study. The extension of the  
 637 Mississippi River and Rio Grande River watersheds are respectively represented in light grey  
 638 and dark grey (Brown et al., 2005; Dahm et al., 2005; Delong, 2005; Galat et al., 2005;  
 639 Matthews et al., 2005; White et al., 2005).  
 640

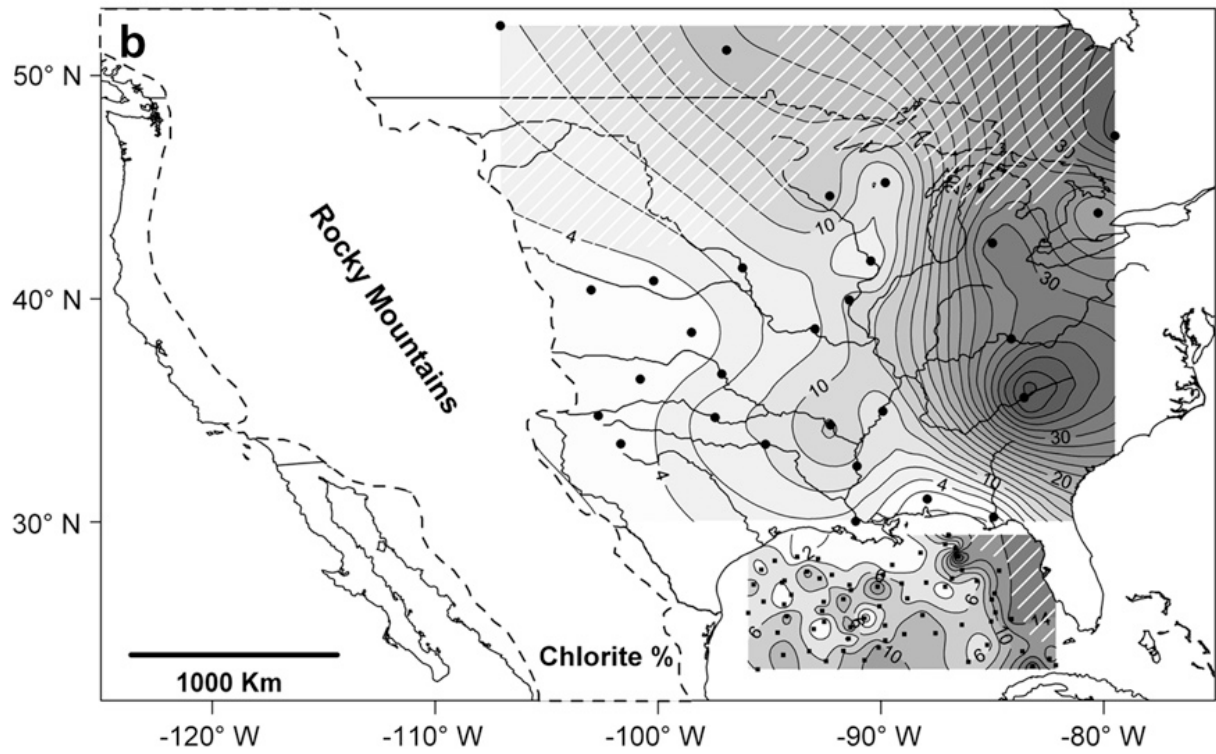
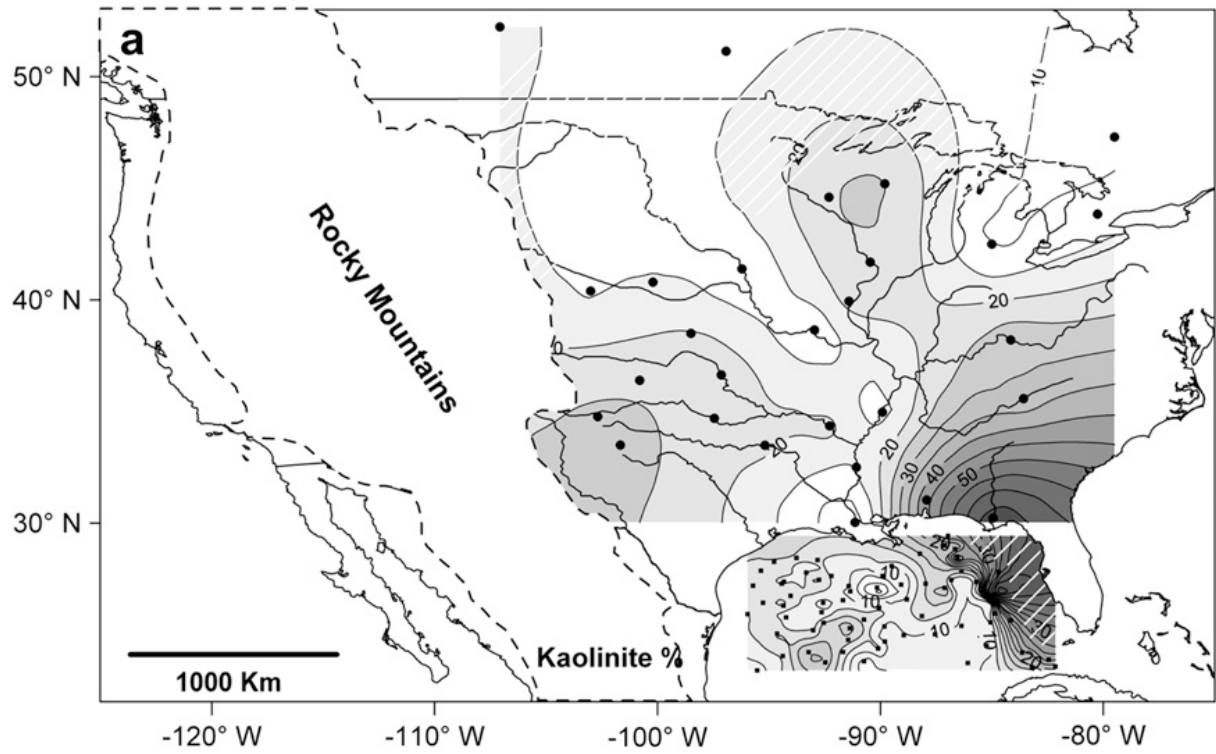


641  
 642 Fig. 5. Location of rivers and main geological provinces (loess province, yellow-red tropical  
 643 soils, Llano Estacado, Appalachians and Rocky Mountains).

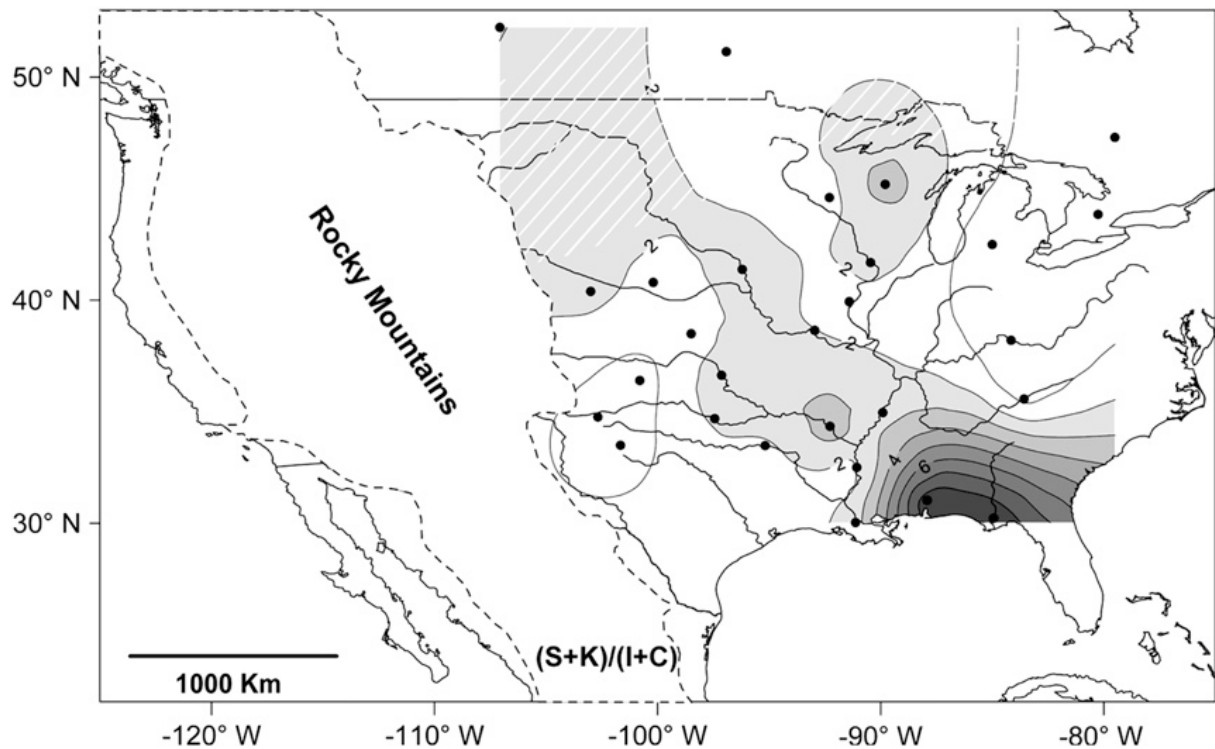


644  
 645 Fig. 6. Distribution of smectite (a) and illite (b) over the North American continent east of the  
 646 Rocky Mountains. White lines indicate areas with larger uncertainties.

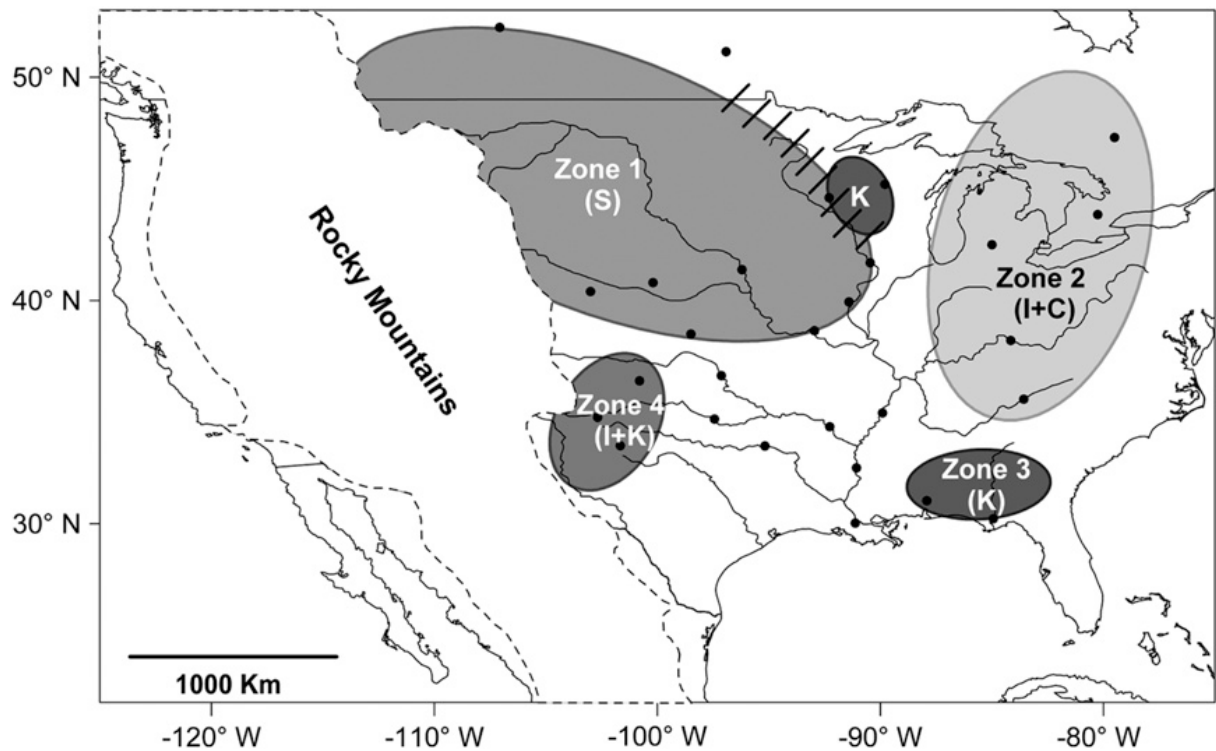
647



648  
 649 Fig. 7. Distribution of kaolinite (a) and chlorite (b) on the studied area. White lines indicate  
 650 areas with larger uncertainties.  
 651



652  
 653 Fig. 8. Distribution of the (smectite + kaolinite)/(illite + chlorite) ratio which indicates the  
 654 type of weathering (chemical or physical) that affected the erodible sediments. High/low  
 655 values of this ratio suggest that chemical/physical weathering prevails in the studied region.  
 656 But the respective contributions of both physical and chemical weathering can not be easily  
 657 deduced in the areas characterized by intermediate values of the  $(S + K)/(I + C)$  ratio. For  
 658 instance, the values observed in Wisconsin (site 7) reflect the presence of kaolinite inherited  
 659 from old saprolite layers. In that case intermediate values of the  $(S + K)/(I + C)$  ratio, cannot  
 660 be interpreted as a weathering index. White lines indicate areas with larger uncertainties.  
 661



662  
 663 Fig. 9. Map of the four major clay mineral provinces over the United States. The smectite-rich  
 664 zone covers a kaolinite-rich area near the Great Lakes (Zone K). Black dashes along the  
 665 northern border of Zone 1 indicate uncertainty in the position of the boundary between this  
 666 zone and Zone K.  
 667

668 Table 1

669 Location, water depth and clay mineral composition of surface sediments from the northern

670 Gulf of Mexico

Site	Core	Latitude	Longitude	Water (m)	Smectite (%)	Illite (%)	Kaolinite (%)	Chlorite (%)
1	MD03-2641	27.29° N	-094.43° W	1427	58	27	11	4
2	MD03-2643	27.37° N	-094.33° W	1379	57	27	12	4
3	MD02-2533/2534	26.74° N	-094.03° W	1350	59	23	14	4
4	MD02-2549	26.43° N	-092.57° W	2049	67	20	9	4
5	MD02-2548	27.64° N	-092.20° W	610	57	28	10	5
6	MD02-2553	27.18° N	-091.42° W	2259	62	23	11	4
7	MD02-2550/2552	26.95° N	-091.35° W	2245	60	25	9	6
8	MD02-2558	28.08° N	-089.49° W	1125	62	25	11	2
9	MD02-2574	28.63° N	-088.22° W	1963	56	25	16	3
10	MD02-2575/2576	29.00° N	-087.12° W	848	60	16	19	5
11	MD02-2577/2578	28.84° N	-086.66° W	476	53	25	18	4
12	MD02-2581	23.88° N	-082.44° W	1063	49	14	26	11
13	AT185-43P	27.78° N	-093.33° W	183	59	23	9	9
14	AT185-58P	27.11° N	-090.15° W	2138	72	15	0	13
15	VM3-7P	23.58° N	-082.15° W	1681	42	25	20	13
16	VM3-9P	27.82° N	-084.70° W	181	34	19	34	13
17	VM3-16P	26.53° N	-085.03° W	3286	62	15	13	10
18	VM3-19P	26.80° N	-084.90° W	730	0	40	48	12
19	VM3-34P	27.10° N	-087.12° W	2889	62	17	19	2
20	VM3-35P	27.37° N	-085.70° W	3221	64	20	11	5
21	VM3-39P	28.45° N	-086.55° W	647	20	30	30	20
22	VM3-42P	29.43° N	-086.97° W	667	32	28	27	13
23	VM3-68P	25.05° N	-094.63° W	3630	55	23	15	7
24	VM3-81P	27.63° N	-089.90° W	1123	57	26	12	5
25	VM3-83P	28.35° N	-092.82° W	149	58	27	12	3
26	VM3-90P	28.45° N	-093.77° W	140	61	24	14	1
27	VM3-93P	27.20° N	-095.72° W	964	52	27	14	7
28	VM3-98P	25.37° N	-089.82° W	3424	67	17	9	7
29	VM3-99P	26.22° N	-090.07° W	3157	54	26	14	6
30	VM3-100P	27.25° N	-089.07° W	2034	67	20	7	6
31	VM3-121P	26.43° N	-095.27° W	1648	54	28	13	5
32	VM3-108P	28.27° N	-094.77° W	148	55	25	14	6
33	VM3-112P	27.87° N	-095.37° W	191	57	27	13	3
34	VM3-114P	27.47° N	-092.75° W	761	44	32	17	7
35	VM3-118P	26.55° N	-091.68° W	2212	51	29	10	10
36	VM3-125P	24.22° N	-093.22° W	3744	43	32	19	6
37	VM3-128P	23.77° N	-092.47° W	3590	53	23	18	6
38	VM3-139P	24.20° N	-083.65° W	1103	41	26	22	11
39	VM3-142P	23.53° N	-083.20° W	1785	42	24	16	18
40	VM17-7P	25.65° N	-084.15° W	154	30	30	25	15
41	VM17-19P	23.82° N	-090.73° W	3706	54	30	6	10
42	VM18-362P	26.58° N	-088.82° W	2577	67	17	11	5
43	RC9-15P	25.56° N	-085.06° W	3341	57	25	10	8
44	RC9-16P	27.85° N	-086.36° W	3111	54	24	13	9
45	RC9-18P	25.29° N	-091.37° W	3374	43	28	18	11
46	RC9-21P	25.93° N	-095.96° W	960	56	27	12	5
47	RC9-22P	26.31° N	-094.35° W	1955	55	28	15	2
48	RC9-23T	26.02° N	-092.63° W	2111	58	25	9	8
49	RC9-24P	25.68° N	-090.74° W	3424	73	14	13	0
50	RC9-25P	24.78° N	-091.45° W	3576	3	24	15	3
51	RC9-31P	23.74° N	-086.08° W	3466	71	13	10	6
52	RC10-267P	24.05° N	-094.38° W	3749	58	20	12	10
53	VM24-19P	27.47° N	-086.82° W	3012	63	19	10	8
54	VM24-20P	27.28° N	-087.97° W	2651	55	26	14	5
55	VM24-21P	24.38° N	-090.10° W	3654	46	30	13	11
56	RC12-5P	25.95° N	-084.87° W	2946	47	27	16	10
57	RC12-4P	24.50° N	-085.23° W	3405	72	15	8	5
58	RC12-8T	25.20° N	-093.02° W	3576	71	15	11	3
59	RC12-9P	25.78° N	-094.23° W	3263	61	21	9	9
60	RC10-10P	23.40° N	-095.53° W	3054	61	24	9	6
61	RC12-13P	24.70° N	-089.80° W	3563	66	19	8	7
62	RC12-14P	25.02° N	-087.55° W	3389	56	26	9	9
63	VM26-131P	25.40° N	-086.37° W	3252	60	23	10	7
64	VM26-132P	24.98° N	-088.95° W	3484	56	25	10	9
65	VM26-138P	25.53° N	-092.55° W	1677	55	28	15	2
66	VM26-141P	24.23° N	-091.68° W	3740	54	25	13	8
67	VM26-142P	25.83° N	-088.13° W	3103	59	19	13	9

671

672

673 Table 2

674 Location, sediment type, number of samples (N) and clay mineral composition of sites from

675 North America

Site	Location	Latitude	Longitude	Type	Smectite (%)	Illite (%)	Kaolinite (%)	Chlorite (%)	Reference
1	Quincy, Illinois	39.94° N	-091.41° W	Loess	39	27	22	11	
2	Saskatchewan	52.23° N	-107.07° W	River	59	17	16	7	
3	Lake Manitoba	51.14° N	-096.92° W	Lake	46	26	13	15	
4	Ottawa River	47.30° N	-079.50° W	River	0	54	8	37	
5	Ontario	43.85° N	-080.26° W	Till	25	43	12	20	
6	St. Francis Lake	42.50° N	-085.00° W	Till	1	58	8	33	
7	Stetsonville	45.20° N	-089.80° W	Till	53	15	26	7	
8	River Falls	44.60° N	-092.30° W	Loess	35	26	25	14	
9	Upper Mississippi River	41.69° N	-090.46° W		45	25	25	5	Potter et al., 1975
10	Kelly section	40.40° N	-103.00° W	Loess	57	26	14	3	
11	Bignell Hill/Eustis sections	40.80° N	-100.20° W	Loess	47	34	16	3	
12	Upper Missouri River	41.38° N	-096.21° W		60	22	11	7	Potter et al., 1975
13	Lower Missouri River	38.65° N	-092.96° W		55	27	11	7	Potter et al., 1975
14	Ohio River	38.21° N	-084.16° W		0	41	29	30	Potter et al., 1975
15	Tennessee River	35.58° N	-083.57° W		0	26	31	43	Potter et al., 1975
16	Barton section	38.50° N	-098.50° W	Loess	35	43	21	2	
17	Texas (Norwood House)	36.40° N	-100.80° W	Dust	14	59	24	2	
18	Arkansas River	36.64° N	-097.14° W		50	21	24	5	Potter et al., 1975
19	Lower Arkansas River	34.35° N	-092.27° W		57	8	22	13	Potter et al., 1975
20	Canadian River	34.69° N	-097.45° W		48	23	21	8	Potter et al., 1975
21	Texas (Hereford)	34.77° N	-102.68° W	Dust	14	56	26	4	
22	Texas (Lubbock)	33.50° N	-101.67° W	Dust	9	60	28	3	
23	Red River	33.49° N	-095.78° W		43	28	21	8	Potter et al., 1975
24	Middle Mississippi River	34.96° N	-089.91° W		60	20	12	8	Potter et al., 1975
25	Mississippi River	32.50° N	-091.07° W		45	30	15	10	Potter et al., 1975
26	Lower Mississippi River	30.04° N	-091.13° W		65 (60-80)	25 (20-30)	5 (+chlorite: 10-20)	5 (minor)	Griffin, 1962
27	Mobile Bay	31.03° N	-087.92° W		45 (40-50)	10 (0-10)	45 (40-50)	0 (trace)	Griffin, 1962
28	Apalachicola River	30.23° N	-084.94° W		20 (0-20)	10 (0-10)	70 (60-80)	0 (trace)	Griffin, 1962

676